

## Article

# Timing of Carbonatite Ultramafic Complexes of the Eastern Sayan Alkaline Province, Siberia: U–Pb (ID–TIMS) Geochronology of Ca–Fe Garnets

Maria V. Stifeeva <sup>1</sup>, Ekaterina B. Salnikova <sup>1,\*</sup>, Valentina B. Savelyeva <sup>2</sup>, Alexander B. Kotov <sup>1</sup>, Yulia V. Danilova <sup>2</sup>, Ekaterina P. Bazarova <sup>2</sup> and Boris S. Danilov <sup>2</sup>

<sup>1</sup> Institute of Precambrian Geology and Geochronology RAS, 199034 St. Petersburg, Russia; stifeeva.maria@yandex.ru (M.V.S.)

<sup>2</sup> Institute of the Earth's Crust SB RAS, 664033 Irkutsk, Russia; vsavel@crust.irk.ru (V.B.S.)

\* Correspondence: katesalnikova@yandex.ru

**Abstract:** In this study, we present the results of U–Pb (ID–TIMS) geochronological studies of calcic garnet from the alkaline ultramafic complexes of Eastern Sayan province (eastern Siberia). New U–Pb ID–TIMS garnet ages obtained from different rocks of Bolshaya Tagna ( $632 \pm 2$  Ma) and Srednaya Zima intrusions ( $624 \pm 5$  Ma), as well as previously published garnet ages of the Belaya Zima complex ( $646 \pm 6$  Ma), allow us to constrain the timing and duration of episodes of alkaline ultramafic magmatism in Eastern Sayan province (619–651 Ma). Variations in the chemical compositions of rocks from three massifs indicate that the parental melts were separated from different magmatic chambers generated during the same episode of mantle melting. This study further highlights garnet U–Pb dating as a potentially robust, high-resolution geochronometer to constrain the evolution of the main pulse of alkaline ultramafic magmatism in the large magmatic provinces.

**Keywords:** Eastern Sayan magmatic province; garnet U–Pb (ID–TIMS); alkaline rocks; carbonatite; Rodinia; Siberian craton; Belaya Zima; Srednaya Zima; Bolshaya Tagna



**Citation:** Stifeeva, M.V.; Salnikova, E.B.; Savelyeva, V.B.; Kotov, A.B.; Danilova, Y.V.; Bazarova, E.P.; Danilov, B.S. Timing of Carbonatite Ultramafic Complexes of the Eastern Sayan Alkaline Province, Siberia: U–Pb (ID–TIMS) Geochronology of Ca–Fe Garnets. *Minerals* **2023**, *13*, 1086. <https://doi.org/10.3390/min13081086>

Academic Editors: Giorgio Garuti, Richard E. Ernst and Hafida El Bilali

Received: 16 May 2023

Revised: 7 August 2023

Accepted: 12 August 2023

Published: 14 August 2023



**Copyright:** © 2023 by the authors. Licensee MDPI, Basel, Switzerland. This article is an open access article distributed under the terms and conditions of the Creative Commons Attribution (CC BY) license (<https://creativecommons.org/licenses/by/4.0/>).

## 1. Introduction

The timing and duration of magmatic events are important factors in understanding the lifespans of plumes and in addressing geodynamic constraints. Alkaline rocks with carbonatites are often temporally and spatially associated with large magmatic provinces (LIP), which are commonly thought to have a very short lifespan (<5 Ma), or to consist of multiple short pulses [1–5] over a longer period of time. However, the problem of timing magmatic events is strongly dependent on the resolution of dating techniques and the quality of the data. The U–Pb zircon method has proven to be of particular usefulness [3,6,7] relative to Rb–Sr, Ar–Ar, and other isotopic systems. Unlike all other chronometers, the U–Pb method is based on two U–Pb decay systems, making it possible to detect even negligible amounts of open system behavior. Zircon demonstrates lattice stability and high U–Pb closure temperatures. Recent studies have focused on the application of the U–Pb system of calcic garnet to precisely date different ages and compositionally diverse alkaline and carbonatitic intrusive rocks and scarns [8–12]. Calcic garnet typically contains enough U for precise age determinations, has a high U–Pb closure temperature (>850 °C) [13], and is resistant to postmagmatic processes. Calcic garnet is a widespread mineral of rocks of the foidolite series, and is therefore a promising source of reliable information about the age of alkaline ultramafic intrusions. The results of a U–Pb (ID–TIMS) geochronological study of calcic garnet from alkaline ultramafic complexes of the Kola Alkaline province (Vuoriyarvi, Sallanlatva, Salmagorsky, and Afrikanda) enable an evaluation of a narrower time span of the main pulse of alkaline ultramafic magmatic activity in Kola province than was previously estimated [14].

This study is an example of attempt to solve the problem of the duration of the Eastern Sayan alkaline magmatic province using a U–Pb system of calcic garnet from ultramafic–alkaline series intrusive rock complexes. The Eastern Sayan rare-metal province is a part of the Neoproterozoic alkaline–carbonatite magmatic area (province) traced for more than 2000 km along the southern margin of the Siberian craton. The alkaline ultrabasic intrusions are concentrated between the southwestern part of the Siberian craton and the Eastern Sayan mountain ridge and distributed along both sides of the Iysko–Urik Graben within the Irkutsk region. The Eastern Sayan province includes the Belaya Zima (Nizhnesayansky), Srednaya Zima (Verkhnesayansky), Bolshaya Tagna, and Bolshezhidosky (Zadoysky) complexes, as well as the Monkresovsky and Yarma fields of dikes of ultrabasic alkaline rocks and carbonatites. The unique Ziminskii rare metal ore district (Nb, Ta, REE, U, Pb, Zn, and P) is related to Eastern Sayan province [15,16]. One of the largest niobium deposits of the province is linked with the Belaya Zima complex, which is the most well-studied complex within the province. Within the past decade, numerous geochronological data have been obtained concerning the age of the Eastern Sayan province complexes, with estimates ranging from 645 to 622 Ma. Thus, available geochronological data (ID–TIMS U–Pb garnet and phlogopite  $^{40}\text{Ar}/^{39}\text{Ar}$ ) have been obtained only for the Belaya Zima complex, with estimates ranging from 622 to 645 Ma (according to ID–TIMS U–Pb analysis [12],  $^{40}\text{Ar}/^{39}\text{Ar}$  dating [17,18], and ID–TIMS U–Pb analysis of zircon [19]). An Sm–Nd isochron age of  $640 \pm 11$  Ma was obtained for rocks of the Bolshaya Tagna complex [20].  $^{40}\text{Ar}/^{39}\text{Ar}$  dating of phlogopites from rocks of the dike series provided two plateaus, with ages of  $644 \pm 9$  and  $646 \pm 9$  Ma [18].

Available geochronological data were obtained using different isotope methods ( $^{40}\text{Ar}/^{39}\text{Ar}$ , Sm–Nd, and U–Pb) with different closure temperatures, making it difficult to determine whether this time span corresponds to the real duration of Neoproterozoic intrusive alkaline magmatism in the province during the interval of ~620–650 Ma, or whether it reflect the effects of isotope system behavior. Therefore, additional geochronological data obtained using modern and precise techniques are required to solve this problem.

The formation of Neoproterozoic alkaline complexes in the southern part of the Siberian platform is associated with the breakup of Rodinia [19]. Hence, determining the duration of the Eastern Sayan magmatic alkaline process is important for the paleogeographic reconstruction of the Siberia–Laurentia connection.

## 2. Analytical Techniques

### 2.1. Whole-Rock Geochemistry

The major elements of whole rock were analyzed at the “Geodynamics and Geochronology Center” at the Institute of the Earth’s crust of the Siberian Branch of the Russian Academy of Sciences (Irkutsk, Russia). Crushed sample was mixed with a combination of soda and boron at a temperature of 950 °C. The resulting alloy was dissolved in hydrochloric acid, the volume was brought to 500 mL with distilled water, and the major elements were determined in aliquots of the resulting solution [21]. The Genesis 10S spectrophotometric complex was used to determine  $\text{SiO}_2$ ,  $\text{TiO}_2$ ,  $\text{Al}_2\text{O}_3$ ,  $\text{Fe}_2\text{O}_3$ ,  $\text{FeO}$ , and  $\text{P}_2\text{O}_5$ , whereas a Solaar M6 atomic absorption spectrophotometer was used to determine  $\text{MnO}$ ,  $\text{CaO}$ ,  $\text{MgO}$ ,  $\text{K}_2\text{O}$ , and  $\text{Na}_2\text{O}$  [22,23]. F was determined using the potentiometric method,  $\text{H}_2\text{O}$  and calcination losses were determined via a gravimetric method, and  $\text{CO}_2$  was determined using the titrimetric method [21]. The accuracy of the analysis of petrogenic oxides was 0.5%–1.0%.

Trace elements and rare earth elements were analyzed using inductively coupled plasma mass spectrometry (ICP-MS) on an Agilent 7900ce analyzer at the “Geodynamics and Geochronology Center” of the Institute of the Earth’s Crust SB RAS (Irkutsk, Russia). The samples were fused with  $\text{LiBO}_2$  using the method developed by the authors of [24]. Calibration was performed according to national and international standards, including G-2, GSP-2, JG-2, and RGM-1. The accuracy of the analysis of the rare and rare earth elements was up to 5%.

## 2.2. Major-Element Garnet Analysis

For a major-element analysis study, we selected three samples of garnet from two alkaline complexes. The garnet crystals were mounted in epoxy, and polished and analyzed at the Geomodel Research Center (Saint-Petersburg State University, Saint-Petersburg, Russia) using a Hitachi S-3400N electron microscope with an Oxford X-Max 20 energy-dispersive analysis attachment. The instrument was operated at 20 kV and 17 nA, with a spectrum-counting time of 30 s. The WDS data were converted to mineral formulas, and the  $\text{Fe}^{2+}/\text{Fe}^{3+}$  ratio was calculated assuming the ideal garnet stoichiometry, i.e., 12 oxygen atoms and 8 cations. The chemical formulas of the garnets and components were calculated according to the method described in [25].

## 2.3. U–Pb ID–TIMS

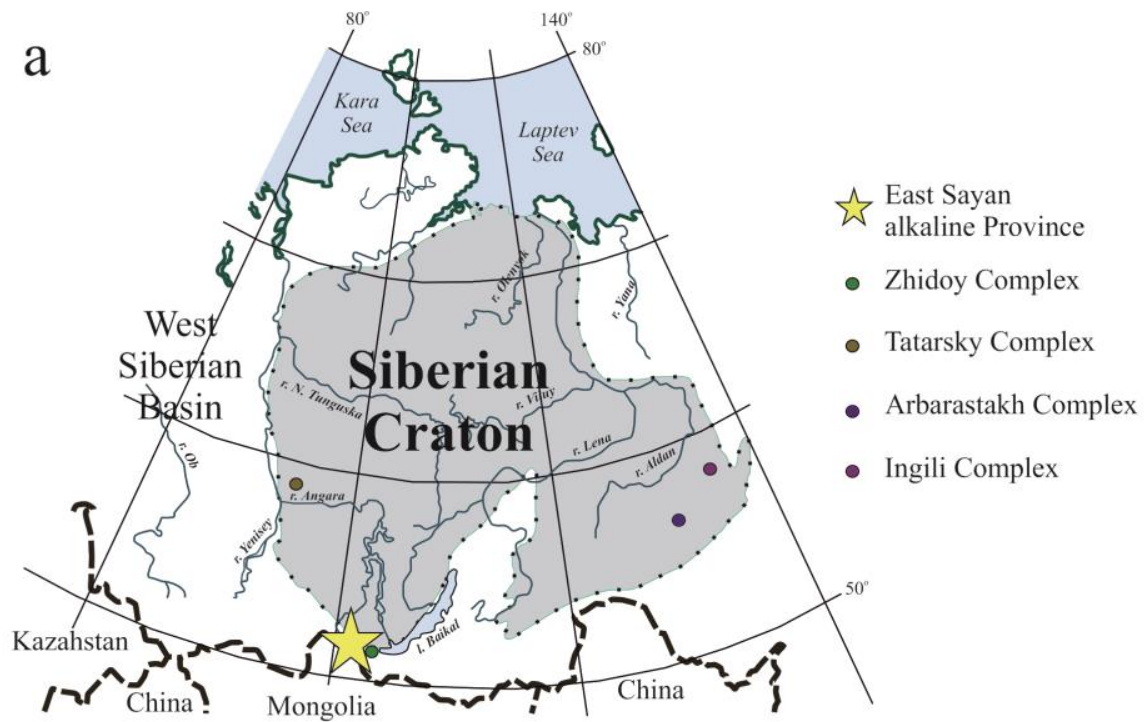
Geochronological studies of garnets using ID–TIMS-based U–Pb were undertaken at the Isotope Geology Laboratory of the Institute of Precambrian Geology and Geochronology (IPGG RAS, Saint-Petersburg, Russia). For this study, we hand-picked the most visually homogeneous single-crystal fragments measuring  $<200\ \mu\text{m}$  in size (2–15 fragments were used for analysis). The selected garnet fractions were subjected to preliminary ultrasonic cleaning with 1 N HCl followed by acid treatment to dissolve calcite and apatite inclusions (6 N HCl at 80 °C for 15–30 min) [26]. Then, the samples were washed in warm water for 20 min, placed in a pressure vessel for digestion [27], spiked with a  $^{202}\text{Pb}$ – $^{235}\text{U}$  tracer, and dissolved in a mixture of 29 N HF and 15 N  $\text{HNO}_3$  (in a proportion of 10:1) at 220 °C for 24–48 h. The Pb and U were separated using a single-stage upgrading technique, which involves the elimination of interfering elements (Ca, Fe, Ti, Al, etc.) with a stepwise combination of 3.1 N HCl and 0.5 N HBr prior to the separation of lead and uranium with 6 N HCl and  $\text{H}_2\text{O}$ , respectively [28]. Furthermore, the U was purified with UTEVA resin [29]. The blanks were 10 pg for Pb and 1 pg for U. The accuracy of the U/Pb ratios and the U and Pb contents was 0.5%, and these used to plot the data points on the concordia diagram and any age calculations. In cases where the error exceeded the established value, the calculated analysis uncertainties were used directly. The data were reduced using PbDAT [30], and visualized using ISOPLOT 3.0 [31] software. A correction for common Pb was applied according to the model developed by Stacey and Kramers [32]; all of the errors are reported here as  $2\sigma$ .

According to research teams, to arbitrarily cut off between young and old ages ranges from 800 Ma to 1600 Ma, we used the  $^{206}\text{Pb}/^{238}\text{U}$  geochronometer for age averaging for the slightly discordant analyses, along with the concordia ages for concordant ones.

## 3. Geological Background, Rock Composition, and Geochemical and Mineralogical Characteristics

The Eastern Sayan province comprises several alkaline–ultrabasic complexes located within the joint zone between the southwestern part of the Siberian Platform and the East Sayan mountain ridge (Figure 1a), and distributed along both sides of the Iysko–Urik Graben [15,16].

The locations of complexes are controlled by the fault system of the northwest strike. Massifs intrude into the Paleoproterozoic shales, and greenschists compose the graben. The intrusive complexes of the Eastern Sayan magmatic province are steeply or vertically oriented as tube-shaped or stock-shaped bodies with oval or round sections. Carbonatite rock occupies about 70% of the total area of some complexes in Eastern Sayan province. The ultramafic–alkaline rock series are represented by pyroxenites and melanocratic series of foidolite (melteigite and ijolite). Most ultramafic alkaline rocks were significantly reworked by carbonatite melt. Due to strong secondary alteration, identification of the primary mineral composition of the alkaline rock series is a complicated task [15,16]. The degree of secondary alteration also depends on the locations of intrusion relative to the controlled structures. The Belaya Zima and Srednaya Zima complexes are located directly in the ridge zone, and the carbonatite magmatic stage in these intrusions is more pronounced [15].



**Srednaya Zima Complex**

**Bolshaya Tagna Complex**

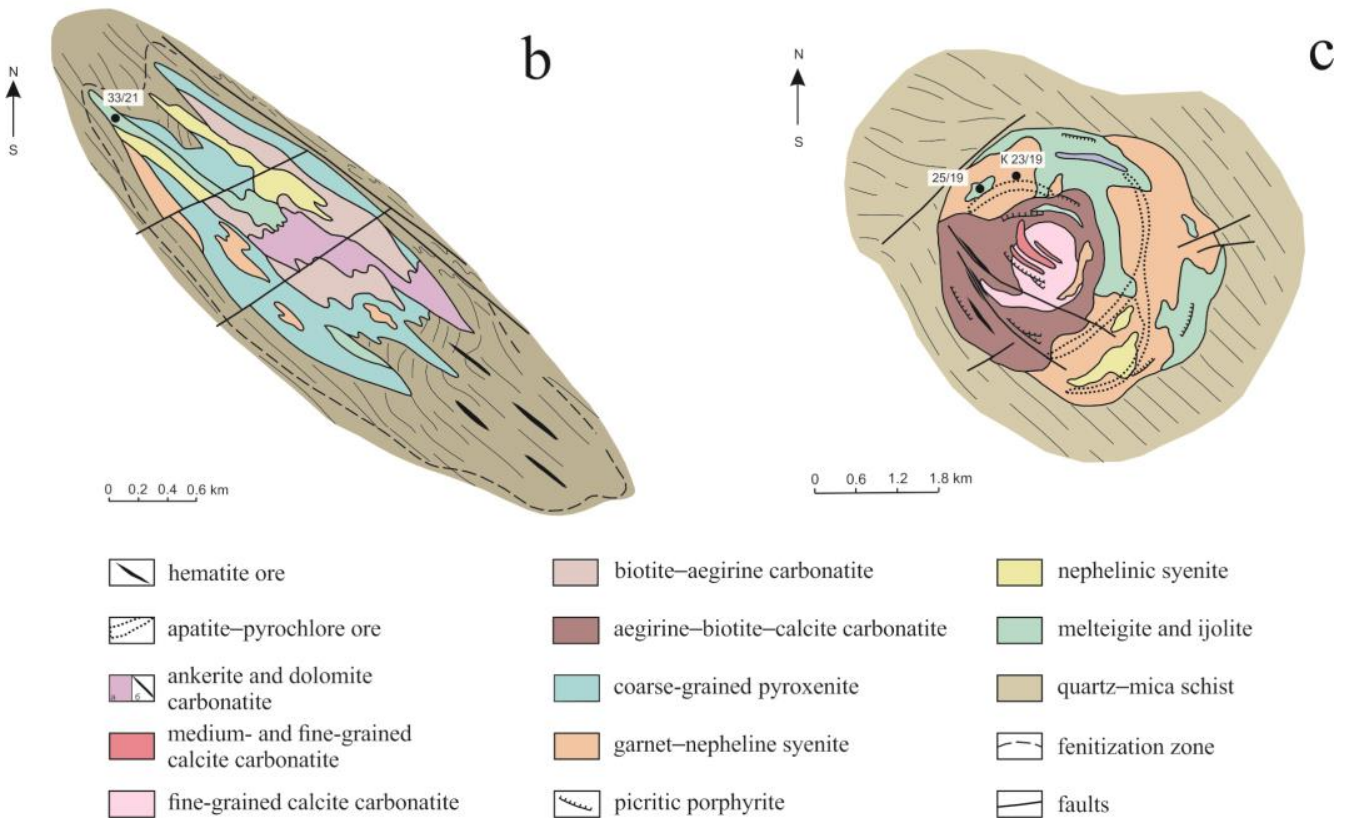


**Figure 1.** (a) The schematic geological maps and locations of the ultramafic–alkaline complexes in the south part of the Siberian craton; (b,c) schematic geological maps of the Srednaya Zima (53°27' N; 100°25' E) and Bolshaya Tagna (53°38' N; 100°28' E) intrusions. The localities of samples for U–Pb study are demonstrated on maps [33].

This province includes several complexes of alkaline ultramafic rocks and dikes of aillkites, mica picrites, kimberlite-like pyroxene-free picrites, lamproites, and rare explosion pipes. These complexes are associated with a rich rare metal Ziminskii ore district.

The Belaya Zima (Beloziminsky) Complex is located on the left bank of the Zima River at the intersection of the Iysko–Urik Graben and the Taimyr–Angara paleo rift. The intrusion crops out over an area of 18 km<sup>2</sup>. Its country rocks are Neoproterozoic schists, quartzites, and dolerite sills [33]. The alkaline intrusive series includes ijolite and nepheline syenites that form arcuated bodies arranged concentrically around a central carbonatite stock. The nepheline syenite has a U–Pb ID–TIMS zircon age of  $643 \pm 4.0$  Ma [19]. The U–Pb ID–TIMS garnet age of calcite-bearing ijolite is  $645 \pm 6$  Ma [12], and the age of an ankerite carbonatite Ar–Ar phlogopite is  $645 \pm 6.0$  Ma [16].

The Sredhaya Zima Complex is located in the Iysko–Urik Graben area, not far from the Belaya Zima Complex. Its country rocks comprise Neoproterozoic sandstones and schists, which are intensively fenitized and complicated in a northwest- and northeast-trending fracture system. The complex has a lenticular form of 2.6 km<sup>2</sup> at the current level of exposure (Figure 1b). The formation of the complex was a multistage process [34]. The earliest intrusion phases are fine-grained pyroxenite, which are preserved as a xenolith in the carbonatitic rocks. The second phase formed series of veins and lenticular bodies of ijolite and melteigite. The rocks of the next phase comprise medium-grained porphyric varieties of syenite. The last alkaline series of rocks is subalkaline massive coarse- and fine-grained syenite. Carbonatitic rocks ended the magmatic evolution of the Srednaya Zima intrusive complex. They occupy more than half the area of the massif. The carbonatite series includes biotite–calcite, aegirine–calcite, aegirine–biotite–calcite, amphibole–calcite, and ankerite–dolomite varieties of rocks, with carbonatitic rocks associated with betafite (main type), pyrochlore, apatite, zircon, burbankite–ancylite, and magnetite mineralization.

The Bolshaya Tagna Complex is surrounded by early Proterozoic metasedimentary rocks. The complex has a circular form with a diameter of approximately 4 km, and is characterized by a concentric zonal structure (Figure 1c) [15,16]. The Bolshaya Tagna intrusion is located away from the East Sayan mountain ridge. The ultramafic–alkaline rocks of this intrusion are relatively less jointed and carbonatized to those in the Belaya Zima and Srednaya Zima intrusions [16]. The alkaline intrusive series is represented by ijolite–melteigite, nepheline syenite, subalkaline feldspathoidal syenite, picrite–porphyrite, and carbonatite (Figure 1c). The most prominent rock variety is ijolite. The less common varieties include nepheline and aegirine syenite. Carbonatite rocks form a large stock body in the western part of the complex and vein-shaped bodies within the alkaline rocks. Carbonatite rock types are stand-out coarse-grained; porphyritic with aegirine, riebeckite, and pyrochlore; and fine-grained calcite–dolomite. Hematite ore in carbonatite and syenite is the final stage of the complex formation.

Ijolite–melteigites from all massifs demonstrate wide variations in chemical composition, whereas alkaline intrusive rocks of the Srednaya Zima complex are very similar in composition to those from the Belaya Zima complex (Figure 2). Most of studied rocks are characterized by relatively low total alkalis due to the presence of calcite in the rocks, which can be both primary magmatic and postmagmatic.

Geochemical studies show that rocks of the alkaline ultramafic complexes are generally characterized by a high content of rare earth elements (Supplementary Materials Table S2). Foidolite series rocks contain 281 to 495 ppm REE, alkaline syenites (81 to 688 ppm REE). The studied rocks demonstrate LREE enrichment, with LREE (La–Eu)/HREE(Gd–Lu) ranging from 5.4 to 94. REE in the spectra, and rock from the Bolshaya Tagna and Srednaya Zima are generally similar to Belaya Zima alkaline silicate rocks (Figure 3) [33].

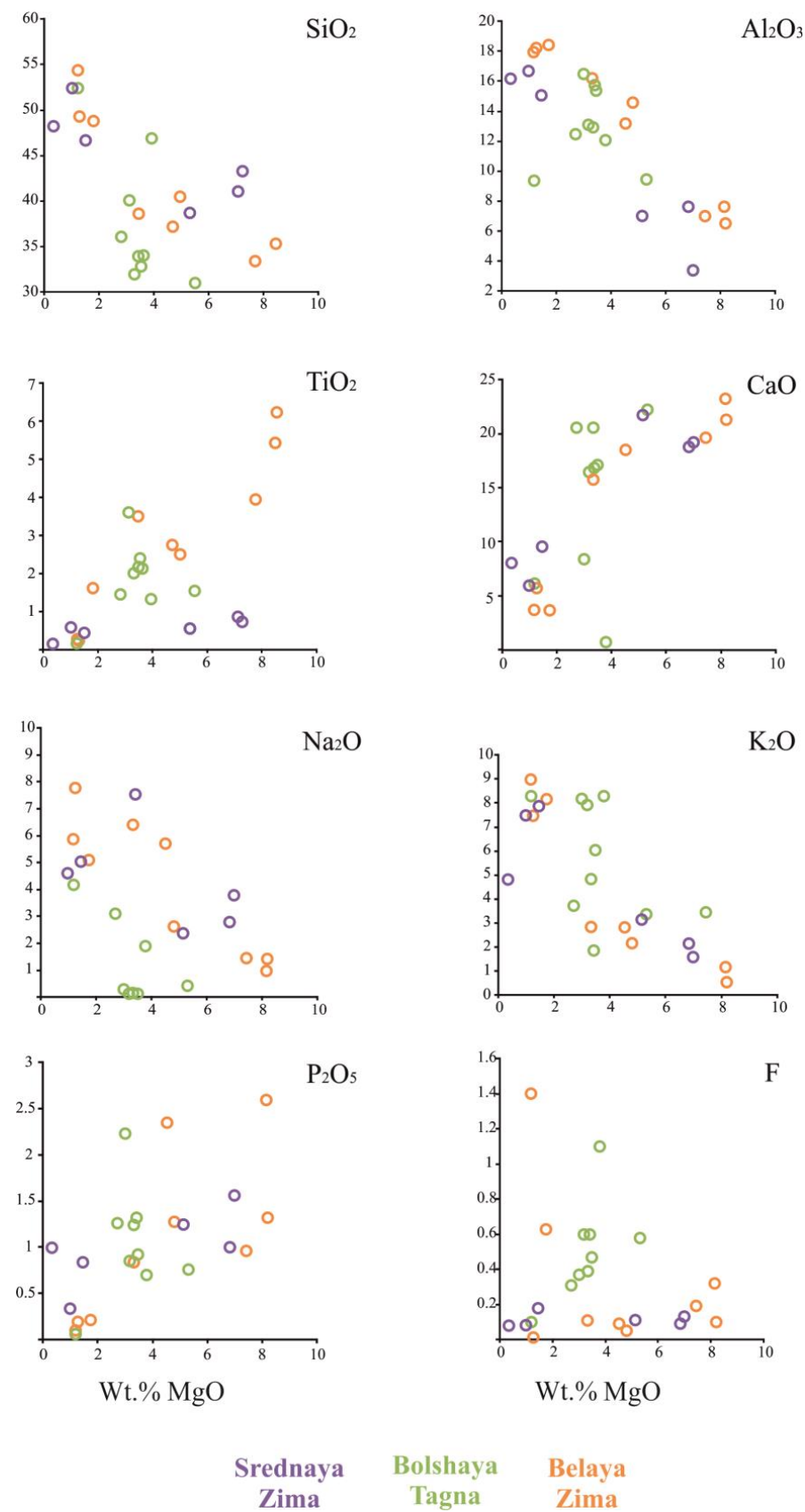


**Figure 2.** MgO variation diagrams for ultramafic-alkaline rock series of Srednaya Zima, Bolshaya Tagna (author’s data), and Belaya Zima complexes [33].

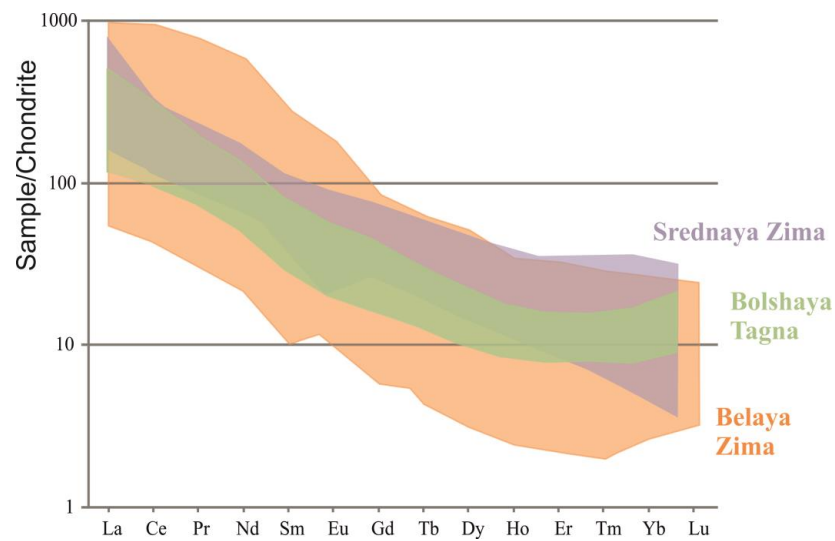


**Figure 3.** Chondrite-normalized REE distribution pattern of ultramafic-alkaline rock series from Srednaya Zima, Bolshaya Tagna (author's data), and Belaya Zima [33]. Normalized values are from [34].

#### 4. Sample Descriptions

##### 4.1. The Srednaya Zima Complex

Garnet is a rare mineral in the Srednaya Zima complex. A garnet sample from calcite-garnet pyroxenite (33/21) was selected for a detailed study. The studied rock contained diopside (60%–65%), calcite (15%–20%), and cancrinite formed on altered nepheline (15%–20%). Biotite (5%–7%), garnet (3%–5%), and aegirine (1%–2%) were less common (Figure 4a). The accessory minerals included fluorapatite, titanite, magnetite, baddeleyite, zircon, Mn-ilmenite, and pyrite.

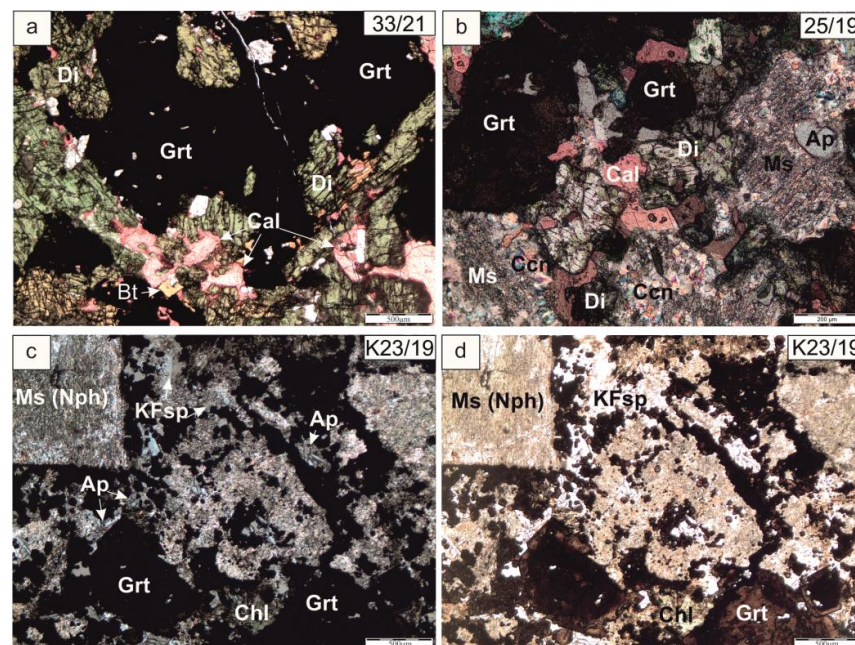


**Figure 4.** Photomicrographs of mineral textures, with polarizing (a,b,d) and crossed (c) nicol; (a) sub-hedral encrustations of garnet in calcite-garnet pyroxenite Srednaya Zima complex (33/21); (b) garnet crystals from altered diopside-garnet ijolite-melteigite (25/19) and zoned garnet (c,d) in altered garnet-nepheline syenite (K23/19) from Bolshaya Tagna complex; Grt—garnet, Ap—apatite, Cal—calcite, Chl—chlorite, Nph—nepheline, KFsp—potassic feldspar, Di—diopside, Ms—muscovite, Bt—biotite, Ccn—cancrinite.

Garnet occurs as subhedral encrustations between diopside, calcite, and pyroxene grains. Some garnet crystals contain single inclusions of apatite and rutile that are located in fractures. The relations between garnet and other rock-forming minerals imply that the garnet formed during the late magmatic stage after diopside, calcite, and biotite.

The color of garnet crystal fragments varies from dark brown to brown. The compositional range of garnet is  $\text{Adr}_{33-48}\text{Mmt}_{21-32}\text{Htn}_{10-15}\text{Sch}_{2-14}\text{Mg-Mmt}_{2-6}$ , with minor proportions of kimzeyite (<3%), Na–Ti garnet (<2.3%), and calderite (<1.3%) (Supplementary Materials Table S1; Figure 5b). No visible zoning was detected in single crystals. The chemical composition of single garnet crystals was found to vary within a narrow range.

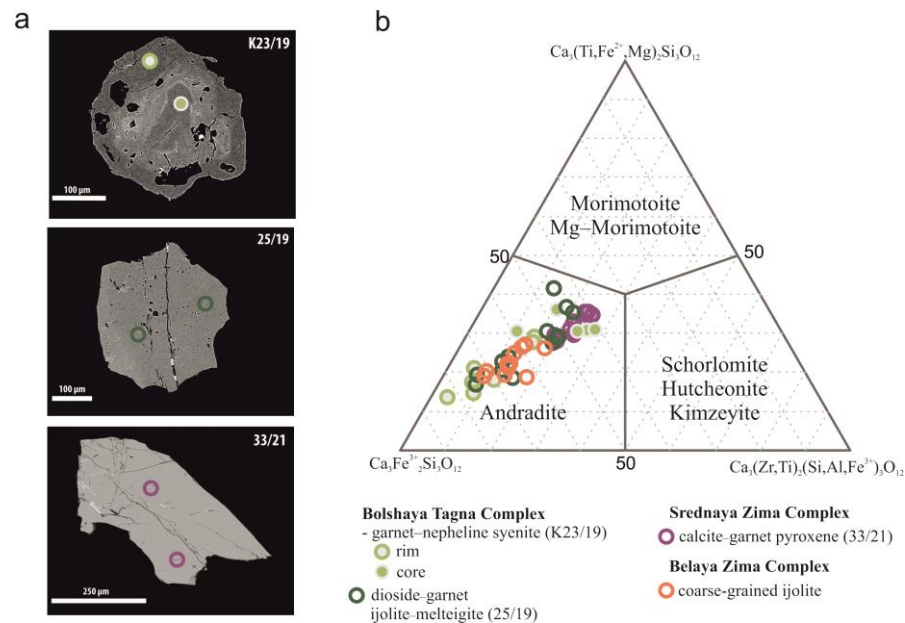


**Figure 5.** (a) Back-scattered electron (BSE) images of garnet crystal from studied rock samples; (b) chemical composition of calcic garnets from the present study and garnet from ijolite from Belaya Zima complex [12], expressed in terms of the principal end-member components (mol.%).

#### 4.2. The Bolshaya Tagna Complex

Garnet samples from altered diopside–garnet, ijolite–melteigite (25/19), and garnet–nepheline syenite (K23/19) were selected for a geochronological study. The ijolite was composed mainly of nepheline (30%–35%), pyroxene (25%–30%), garnet (25%–30%), and calcite (10%–15%) (Figure 4b). The accessory minerals included cancrinite, potassic feldspar, and muscovite. Garnet forms single crystals, and presents as an inclusion in pyroxene grains. Some garnet crystals contain rare inclusions of calcite, apatite, and magnetite. The relationship between minerals in ijolite–melteigite rock indicates that the crystallization of garnet was a synchronous process with diopside that finished after the formation of nepheline, with an average composition of  $\text{Adr}_{45-67}\text{Htn}_{8-14}\text{Mmt}_{15-30}$  (calderite (<1.3%)) (Supplementary Materials Table S1; Figure 5b).

Garnet–nepheline syenite is a porphyritic rock composed of large (0.3–0.6 cm) porphyritic crystals of nepheline (30%–35%) and xenomorphic grains of potassic feldspar (20%–25%), garnet (25%–30%), and pyroxene (10%–15%) (Figure 4c,d). Nepheline crystals are replaced by fine-grained sericite. Garnet forms crystals of a dark brown color up to 1 mm. The composition of garnet ranges from  $\text{Adr}_{38}\text{Mmt}_{13}\text{Sch}_2$  to  $\text{Adr}_{78}\text{Mrt}_{33}\text{Sch}_{23}$ , and the contents of other components (calderite, goldmanite, Na–Ti garnet, kimzeyite, and hutcheonite) do not exceed 5% (calderite (<1.3%)) (Supplementary Materials Table S1; Figure 5b). The garnet crystals are zoned; the abundances of Ti and Zr decrease, whereas Fe and Mn contents increase from the core outward. Some crystals contain inclusions of biotite, calcite, and magnetite. Garnet is partly replaced by Mn-ilmenite.

### 5. Results of U–Pb ID–TIMS Garnet Geochronological Study

#### 5.1. The Srednaya Zima Complex

Andradite from Srednaya Zima calcite–garnet pyroxenite was used for a U–Pb geochronological study. In total, three garnet fractions were selected for analysis (analyses 1–3, Table 1; Figure 6a). The studied samples were characterized by high U contents (8–10 ppm) and low levels of common Pb ( $Pb_c/Pb_t = 0.1–0.2$ ). The data points were concordant (#2 and 3, Table 1) or slightly discordant (#1, Table 1), and yielded a concordia age of  $624 \pm 5$  Ma (MSWD = 0.31, the probability of concordance = 0.58). The weighted average of  $^{206}Pb/^{238}U$  ages of all analyzed garnet fractions (#1–3, Table 1) corresponded to an age of  $623 \pm 5$  (MSWD = 1.6), which is close to the concordia age (Figure 6c). However, the obtained U–Pb garnet age is the first geochronological data to be reported for the Srednaya Zima complex.

**Table 1.** U–Pb ID–TIMS isotopic data <sup>a</sup> for garnets from ultramafic–alkaline rocks of the Eastern Sayan province.

No.	Garnet Characteristic; Treatment Type	Weight, mg	Pb, ppm	U, ppm	Pbc/Pbt	$^{206}Pb/^{204}Pb$ <sup>b</sup>	Isotopic Ratios Corrected for Blank and Common Pb				Rho	Age, Ma		
							$^{207}Pb/^{206}Pb$	$^{208}Pb/^{206}Pb$	$^{207}Pb/^{235}U$	$^{206}Pb/^{238}U$		$^{207}Pb/^{235}U$	$^{206}Pb/^{238}U$	$^{207}Pb/^{206}Pb$
Srednaya Zima Complex														
calcite-garnet pyroxenite (33/21)														
1	Fragments; 6–8 N HCl	0.44	1.87	9.99	0.13	202	$0.0611 \pm 2$	$0.8311 \pm 1$	$0.8537 \pm 34$	$0.1013 \pm 2$	0.60	$627 \pm 2$	$622 \pm 1$	$644 \pm 7$
2	Fragments; 6–8 N HCl	0.42	1.77	8.71	0.20	135	$0.0608 \pm 2$	$0.7986 \pm 1$	$0.8537 \pm 42$	$0.1019 \pm 3$	0.58	$627 \pm 3$	$625 \pm 2$	$632 \pm 9$
3	Fragments; 6–8 N HCl	1.20	1.43	8.28	0.07	368	$0.0604 \pm 3$	$0.7775 \pm 1$	$0.8439 \pm 48$	$0.1013 \pm 2$	0.46	$621 \pm 4$	$622 \pm 1$	$619 \pm 11$
Bolshaya Tagna Complex														
altered garnet-nepheline syenite (23/19)														
4	Fragments; 6–8 N HCl	0.94	0.89	5.24	0.42	88	$0.0614 \pm 3$	$0.0457 \pm 1$	$0.8752 \pm 51$	$0.1033 \pm 2$	0.48	$638 \pm 4$	$634 \pm 1$	$655 \pm 11$
5	Fragments; 6–8 N HCl	0.95	0.93	4.71	0.50	76	$0.0617 \pm 3$	$0.0499 \pm 1$	$0.8783 \pm 46$	$0.1032 \pm 2$	0.55	$640 \pm 3$	$633 \pm 2$	$664 \pm 9$
6	Fragments; 6–8 N HCl	0.78	0.61	3.18	0.49	71	$0.0607 \pm 5$	$0.0324 \pm 1$	$0.8633 \pm 93$	$0.1031 \pm 6$	0.60	$632 \pm 7$	$632 \pm 4$	$630 \pm 19$
altered diopside-garnet ijolite-melteigite (25/19)														
7	Fragments; 6–8 N HCl	0.34	0.70	4.64	0.29	77	$0.0617 \pm 11$	$0.1377 \pm 1$	$0.8757 \pm 183$	$0.1029 \pm 9$	0.50	$639 \pm 13$	$631 \pm 5$	$665 \pm 39$
8	Fragments; 6–8 N HCl	0.40	0.64	2.70	0.53	60	$0.0609 \pm 5$	$0.2009 \pm 1$	$0.8643 \pm 86$	$0.1029 \pm 3$	0.45	$632 \pm 6$	$632 \pm 2$	$635 \pm 19$
9	Fragments; 6–8 N HCl	0.55	0.73	4.58	0.33	106	$0.0631 \pm 5$	$0.1414 \pm 1$	$0.8999 \pm 92$	$0.1033 \pm 4$	0.51	$652 \pm 7$	$634 \pm 3$	$713 \pm 19$

<sup>a</sup> All measured values are given to the last significant digit (based on the corresponding 2σ). <sup>b</sup> Measured isotopic ratios.

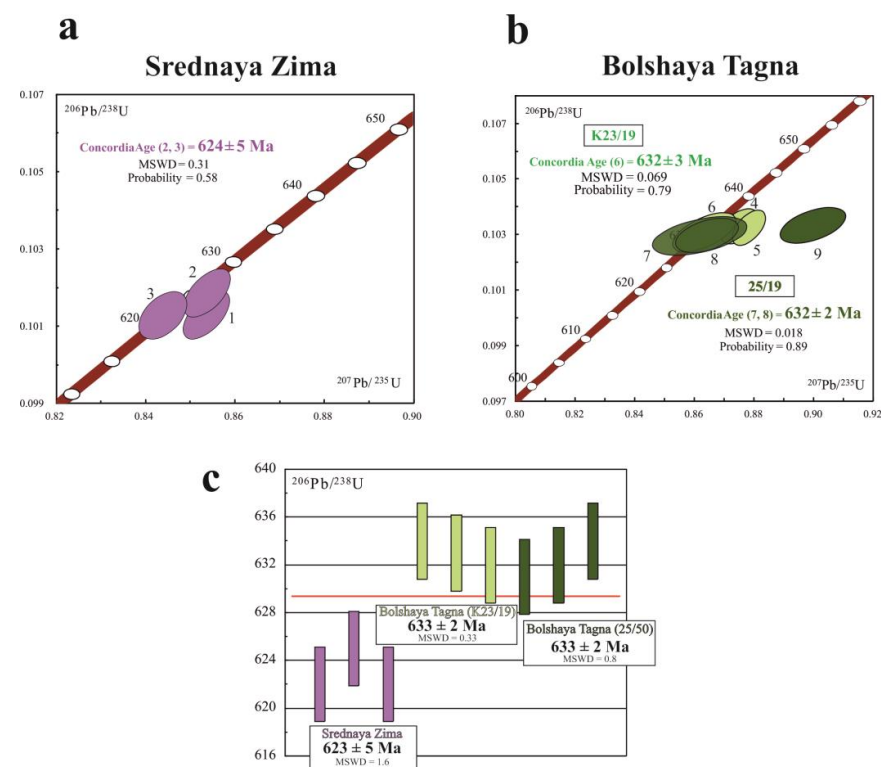


**Figure 6.** Concordia diagrams showing U–Pb ID–TIMS data for calcic garnet from (a) Srednaya Zima and (b) Bolshaya Tagna complexes; (c) weighted average  $^{206}Pb/^{238}U$  for all data points. For the source data, see Table 1. Error ellipses are 2σ.

### 5.2. The Bolshaya Tagna Complex

For the U–Pb geochronological studies, we used visually homogeneous and clean fragments (0.10–0.15 mm) of andradite crystals from altered diopside–garnet ijolite–melteigite (sample 25/19) and altered garnet–nepheline syenite (sample 23/19). The garnet from both samples (analyses 4–9 in Table 1) is characterized by moderate U and low Pb contents (2.7–5.2 and 0.6–0.9 ppm, respectively). The data points of andradite from the ijolites (sample 23/19) were plotted on the concordia (analysis 6, Table 1) or slightly to the right, and yield a weighted average ( $^{206}\text{Pb}/^{238}\text{U}$ ) age of  $633 \pm 2$  (MSWD = 0.33) (#4–6, Table 1; Figure 6c) and a concordia age of  $632 \pm 3$  (MSWD = 0.07, probability = 0.79).

As shown in Figure 6b, two points of the andradite from the nepheline syenite are located on the concordia (analyses 7,8; Table 1), providing a reasonably well-constrained age of  $632 \pm 2$  (MSWD = 0.02; probability of concordance = 0.89). One analysis (#9) is discordant, and reveals some degree of inheritance ( $^{207}\text{Pb}/^{206}\text{Pb} = 713$  Ma). However, the  $^{206}\text{Pb}/^{238}\text{U}$  age of the discordant data point coincides with the concordia age. The weighted average ( $^{206}\text{Pb}/^{238}\text{U}$ ) age of the analyzed garnet fractions from this sample is  $633 \pm 2$  (MSWD = 0.8), which perfectly coincides to the age of the garnet from the ijolite (Figure 6c).

These values reported above are in agreement with (but with more precision) the Sm–Nd age determinations ( $640 \pm 11$  Ma) for the rocks of the Bolshaya Tagna.

## 6. Discussion and Conclusions

Within the southern and southwestern margins of the Siberian craton, the final stages of the breakup of Rodinia are marked by the generation of alkaline ultramafic complexes from 650 to 621 Ma. These complexes trace for more than 3000 km [35] from the Aldan Shield (Arbarastakh and Ingili complexes) through the Altai–Sayan (Bolshaya Tagna, Belaya Zima, Srednaya Zima, and Zhidoy complexes) to the Tatrsky complex (Figure 1a), and are mostly characterized by similar types of rare metal deposits. The timing of Neoproterozoic magmatic events that occurred along the Siberian craton margin is an important point for the geodynamic correlation of the ultimate phase of Rodinia and the early stages of the Paleo-Asian Ocean. The main factors limiting these correlations are geochronological data obtained by different isotopic systems ( $^{40}\text{Ar}/^{39}\text{Ar}$ , K–Ar, U–Pb, and Sm–Nd) for intrusions with carbonatites and ultrabasic dikes.

Numerous recent studies have convincingly shown that Ca–Fe–Ti garnets offer unique opportunities for the timing of magmatic events, with a temporal resolution comparable to that of zircon dating. In this study, we presented new U–Pb (ID–TIMS) geochronological and geochemical data for Ca–Fe–Ti garnets from two complexes of the Eastern Sayan magmatic province and whole-rock geochemistry. Combining new geochronological data with those previously published for the Belaya Zima complex ( $645 \pm 6$  Ma), we provide information on the duration of the main magmatic event and the timing of alkaline ultrabasic complexes of the Ziminsky ore district of emplacement (Figure 1a). The new data provide an age range (ca. 650–624 Ma) with the possible relative age order Belaya Zima (ca. 650 Ma), Bolshaya Tagna (ca. 633 Ma), and Srednaya Zima (ca. 624 Ma). No geochronological data for the latter complex were available before our study. As demonstrated in Figure 7, the precision and accuracy of our U–Pb garnet geochronological study are similar to those using U–Pb zircon age determination, allowing us to evaluate the pulses of magmatic activity within the Eastern Sayan province.

Variations in the chemical composition of rocks from three complexes indicate that the parental melts were separated from different magmatic chambers that were generated during the same episode of mantle melting. According to the  $^{40}\text{Ar}/^{39}\text{Ar}$  phlogopite data obtained for aillikite, damtjernite, and picrite from basic dikes from the northern part of the Eastern Sayan province (650–620 Ma), the rock formation in the dike complex of the region was related to the same stage.

This time span of about 25 Ma is also related to the emplacement of other massifs of biotite pyroxenite, ijolite, urtite, alkaline syenite, and carbonatites within the southern and southwestern marginal parts of the Siberia and Zhidoy complexes ( $632 \pm 2$  Ma [19]),

the Arbarastakh complex (650–638 Ma [36]), the Ingili complex ( $654 \pm 7$  Ma [19]), and the Tatarsky complex (630 Ma [37,38]). At the same time, Neoproterozoic mafic dike swarms within the southeastern and southern parts of the Siberian craton were emplaced about 100 Ma earlier, between 725 and 710 Ma [35,39,40], and demonstrated that at 720 Ma, the center of the Irkutsk plume occurred within the studied area, providing very good correlations with the 720 Ma Franklin plume center of northern Laurentia. The 720 Ma Franklin–Irkutsk LIP event marks an attempted initial separation of southern Siberia from northern Laurentia during the breakup of Rodinia.

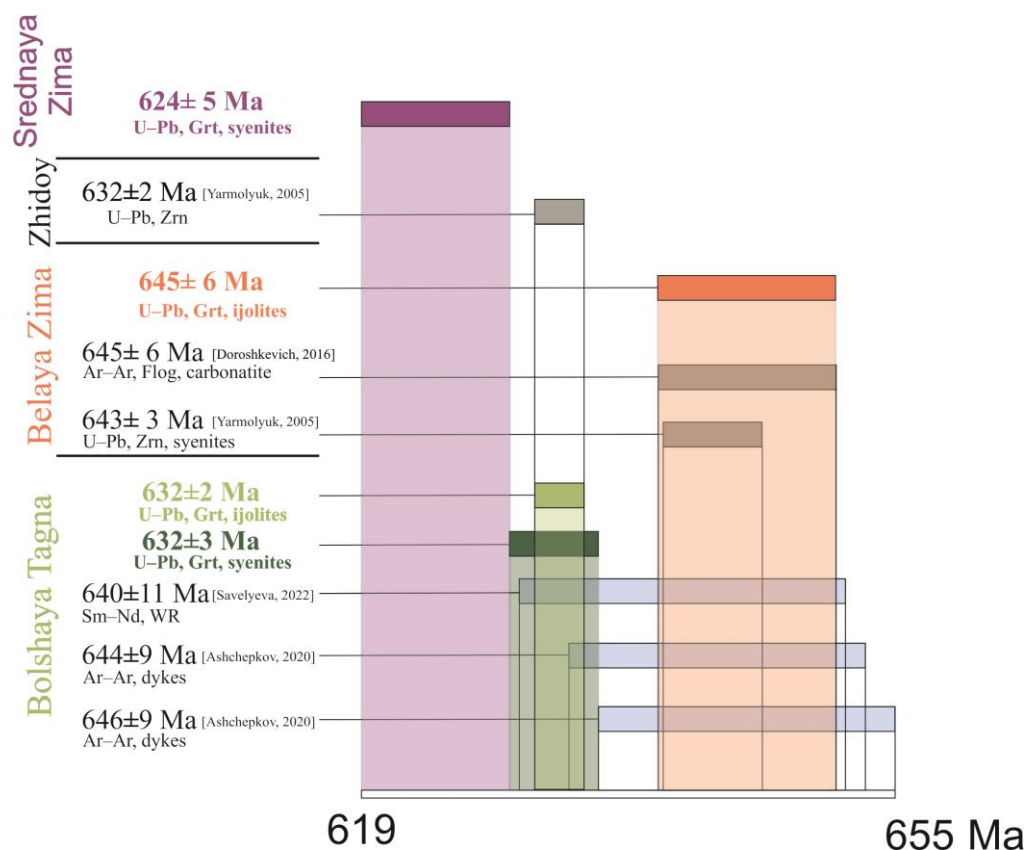


**Figure 7.** Summarized geochronological data for complexes of the Eastern Sayan magmatic province. Used own results and data from [17–20].

Accordingly, basic dikes indicate the early stage of Neoproterozoic extension, while alkaline–ultramafic carbonatitic complexes and potassium dikes record the late stages of extension of the lithosphere, and mark the early stages of the creation of the Paleo-Asian Ocean.

**Supplementary Materials:** The following supporting information can be downloaded at: <https://www.mdpi.com/article/10.3390/min13081086/s1>, Table S1: Chemical analyses of garnets from studied alkaline rocks; Table S2: Chemical composition of ultramafic-alkaline rock series of Srednaya Zima and Bolshaya Tagna complexes.

**Author Contributions:** Conceptualization and writing, M.V.S., E.B.S. and V.B.S.; investigation and U–Pb dating, M.V.S. and E.B.S.; geological background and geochemical study, Y.V.D., E.P.B. and B.S.D.; supervision, A.B.K. All authors have read and agreed to the published version of the manuscript.

**Funding:** This research was supported financially by the Russian Science Foundation (projects nos. 22–17–00211; IPGG theme nos. FMUW-2022-0003) and the “Geodynamic and geochronology” Collective Use Center of the Institute of Earth Crust SB RAS (project nos. 075-15-2021-682).

**Data Availability Statement:** Data will be made available on request.

**Acknowledgments:** We would like to thank the anonymous reviewers and academic editors for their constructive and thorough comments which greatly helped improve the manuscript.

**Conflicts of Interest:** The authors declare no conflict of interest.

## References

1. Ernst, R.E.; Buchan, K.L. Large mafic magmatic events through time and links to mantle plume heads. In *Mantle Plumes: Their Identification through Time*; Ernst, R.E., Buchan, K.L., Eds.; Geological Society of America: Boulder, CO, USA, 2001; Volume 352, pp. 483–575. ISBN 9780813723525.
2. Hofmann, C.; Féraud, G.; Courtillot, V.  $^{40}\text{Ar}/^{39}\text{Ar}$  Dating of Mineral Separates and Whole Rocks from the Western Ghats Lava Pile: Further Constraints on Duration and Age of the Deccan Traps. *Earth Planet. Sci. Lett.* **2000**, *180*, 13–27. [[CrossRef](#)]
3. Courtillot, V.E.; Renne, P.R. On the Ages of Flood Basalt Events. *Comptes Rendus Geosci.* **2003**, *335*, 113–140. [[CrossRef](#)]
4. Jerram, D.A.; Widdowson, M. The Anatomy of Continental Flood Basalt Provinces: Geological Constraints on the Processes and Products of Flood Volcanism. *Lithos* **2005**, *79*, 385–405. [[CrossRef](#)]
5. Blackburn, T.J.; Olsen, P.E.; Bowring, S.A.; McLean, N.M.; Kent, D.V.; Puffer, J.; McHone, G.; Rasbury, E.T.; Et-Touhami, M. Zircon U-Pb Geochronology Links the End-Triassic Extinction with the Central Atlantic Magmatic Province. *Science* **2013**, *340*, 941–945. [[CrossRef](#)] [[PubMed](#)]
6. Heaman, L.M.; LeCheminant, A.N. Paragenesis and U-Pb Systematics of Baddeleyite ( $\text{ZrO}_2$ ). *Chem. Geol.* **1993**, *110*, 95–126. [[CrossRef](#)]
7. Söderlund, U.; Ibanez-Mejia, M.; El Bahat, A.; Ernst, R.E.; Ikenne, M.; Soulaïmani, A.; Youbi, N.; Cousens, B.; El Janati, M.; Hafid, A. Reply to Comment on “U-Pb Baddeleyite Ages and Geochemistry of Dolerite Dykes in the Bas-Drâa Inlier of the Anti-Atlas of Morocco: Newly Identified 1380Ma Event in the West African Craton” by André Michard and Dominique Gasquet. *Lithos* **2013**, *174*, 101–108. [[CrossRef](#)]
8. Salnikova, E.B.; Stifeeva, M.V.; Chakhmouradian, A.R.; Glebovitsky, V.A.; Reguir, E.P. The U-Pb System in Schorlomite from Calcite-Amphobole-Pyroxene Pegmatite of the Afrikanda Complex (Kola Peninsula). *Dokl. Earth Sci.* **2018**, *478*, 148–151. [[CrossRef](#)]
9. Stifeeva, M.V.; Salnikova, E.B.; Samsonov, A.V.; Kotov, A.B.; Gritsenko, Y.D. Garnet U-Pb Age of Skarns from Dashkesan Deposit (Lesser Caucasus). *Dokl. Earth Sci.* **2019**, *487*, 953–956. [[CrossRef](#)]
10. Salnikova, E.B.; Stifeeva, M.V.; Nikiforov, A.V.; Yarmolyuk, V.V.; Kotov, A.B.; Anisimova, I.V.; Sugorakova, A.M.; Vrublevskii, V.V. Andradite-Morimotoite Garnets as Promising U-Pb Geochronometers for Dating Ultrabasic Alkaline Rocks. *Dokl. Earth Sci.* **2018**, *480*, 778–782. [[CrossRef](#)]
11. Stifeeva, M.V.; Vladyskin, N.V.; Kotov, A.B.; Salnikova, E.B.; Sotnikova, I.A.; Adamskaya, E.V.; Kovach, V.P.; Plotkina, Y.V.; Tolmacheva, E.V.; Alymova, N.V. Formation Age of Early Precambrian Carbonatites in the Southeastern Part of the Chara-Olyokma Geoblock, Aldan Shield. *Dokl. Earth Sci.* **2022**, *507*, S247–S250. [[CrossRef](#)]
12. Salnikova, E.B.; Chakhmouradian, A.R.; Stifeeva, M.V.; Reguir, E.P.; Kotov, A.B.; Gritsenko, Y.D.; Nikiforov, A.V. Calcic Garnets as a Geochronological and Petrogenetic Tool Applicable to a Wide Variety of Rocks. *Lithos* **2019**, *338–339*, 141–154. [[CrossRef](#)]
13. Mezger, K.; Hanson, G.N.; Bohlen, S.R. Contributions to Mineralogy and Petrology U-Pb Systematics of Garnet: Dating the Growth of Garnet in the Late Archean Pikwitonei Granulite Domain at Cauchon and Natawahunan Lakes, Manitoba, Canada. *Contrib. Mineral. Petrol.* **1989**, *101*, 136–148. [[CrossRef](#)]
14. Stifeeva, M.V.; Salnikova, E.B.; Arzamastsev, A.A.; Kotov, A.B.; Grozdev, V.Y. Calcic Garnets as a Source of Information on the Age of Ultramafic Alkaline Intrusions in the Kola Magmatic Province. *Petrology* **2020**, *28*, 62–72. [[CrossRef](#)]
15. Frolov, A.A.; Belov, C.V. The Complex Carbonatite Deposits of the Ziminski Ore District (Eastern Sayan, Russia). *Geol. Ore Depos.* **1999**, *41*, 94–113.
16. Frolov, A.A.; Tolstov, A.P.; Belov, C.V. *Carbonatite Deposits of Russia*; NIA-Priroda: Moscow, Russia, 2003.
17. Doroshkevich, A.G.; Veksler, I.V.; Izbrodin, I.A.; Ripp, G.S.; Khromova, E.A.; Posokhov, V.F.; Travin, A.V.; Vladyskin, N.V. Stable Isotope Composition of Minerals in the Belaya Zima Plutonic Complex, Russia: Implications for the Sources of the Parental Magma and Metasomatizing Fluids. *J. Asian Earth Sci.* **2016**, *116*, 81–96. [[CrossRef](#)]
18. Ashchepkov, I.; Zhmodik, S.; Belyanin, D.; Kiseleva, O.N.; Medvedev, N.; Travin, A.; Yudin, D.; Karmanov, N.S.; Downes, H. Aillikites and Alkali Ultramafic Lamprophyres of the Beloziminsky Alkaline Ultrabasic-Carbonatite Massif: Possible Origin and Relations with Ore Deposits. *Minerals* **2020**, *10*, 404. [[CrossRef](#)]
19. Yarmolyuk, V.V.; Kovalenko, V.I.; Salnikova, E.B.; Nikiforov, A.V.; Kotov, A.B.; Vladyskin, N.V. Late Riphean Rifting and Breakup of Laurasia: Data on Geochronological Studies of Ultramafic Alkaline Complexes in the Southern Framing of the Siberian Craton. *Dokl. Earth Sci.* **2005**, *3*, 400–406.
20. Savelyeva, V.B.; Danilova, Y.V.; Letnikov, F.A.; Demonterova, E.I.; Yudin, D.S.; Bazarova, E.P.; Danilov, B.S.; Sharygin, I.S. Age and Melt Sources of Ultramafic Dykes and Rocks of the Bolshetagninskii Alkaline Carbonatite Massif (Urik-Iya Graben, SW Margin of the Siberian Craton). *Dokl. Earth Sci.* **2022**, *505*, 452–458. [[CrossRef](#)]
21. Sizykh, Y.I. *Complex Scheme of Chemical Analysis of Rocks and Minerals*; Institute of Crustal Research, Russian Academy of Sciences: Irkutsk, Russia, 1985.

22. Revenko, A.G. Physical and Chemical Methods of Researching Rocks and Minerals in the Analytical Centre of the Institute of the Earth's Crust, SB RAS. *Geodyn. Tectonophys.* **2014**, *5*, 101–114. [[CrossRef](#)]
23. Ivanov, A.V.; Demonterova, E.I.; Revenko, A.G.; Sharygin, I.S.; Kozyreva, E.A.; Alexeev, S.V. History and Current State of Analytical Research at the Institute of the Earth's Crust SB RAS: Centre for Geodynamics and Geochronology. *Geodyn. Tectonophys.* **2022**, *13*, 0582. [[CrossRef](#)]
24. Panteeva, S.V.; Gladkochub, D.P.; Donskaya, T.V.; Markova, V.V.; Sandimirova, G.P. Determination of 24 Trace Elements in Felsic Rocks by Inductively Coupled Plasma Mass Spectrometry after Lithium Metaborate Fusion. *Spectrochim. Acta Part B At. Spectrosc.* **2003**, *58*, 341–350. [[CrossRef](#)]
25. Bulakh, A.G. *Calculation of Mineral Formulas*, 2nd ed.; Nedra: Moscow, Russia, 1964.
26. Dewolf, C.P.; Zeissler, C.J.; Halliday, A.N.; Mezger, K.; Essene, E.J. The Role of Inclusions in U-Pb and Sm-Nd Garnet Geochronology: Stepwise Dissolution Experiments and Trace Uranium Mapping by Fission Track Analysis. *Geochim. Cosmochim. Acta* **1996**, *60*, 121–134. [[CrossRef](#)]
27. Krogh, T.E. A Low-Contamination Method for Hydrothermal Decomposition of Zircon and Extraction of U and Pb for Isotopic Age Determinations. *Geochim. Cosmochim. Acta* **1973**, *37*, 485–494. [[CrossRef](#)]
28. Corfu, F.; Andersen, T.B. U–Pb Ages of the Dalsfjord Complex, SW Norway, and Their Bearing on the Correlation of Allochthonous Crystalline Segments of the Scandinavian Caledonides. *Int. J. Earth Sci.* **2002**, *91*, 955–963. [[CrossRef](#)]
29. Horwitz, E.P.; Dietz, M.L.; Chiarizia, R.; Diamond, H.; Essling, A.M.; Graczyk, D. Separation and Preconcentration of Uranium from Acidic Media by Extraction Chromatography. *Anal. Chim. Acta* **1992**, *266*, 25–37. [[CrossRef](#)]
30. Ludwig, K.R. *ISOPLOT for MS-DOS, a Plotting and Regression Program for Radiogenic-Isotope Data, for IBM-PC Compatible Computers, Version 1.00*; US Geological Survey: Reston, VA, USA, 1988.
31. Ludwig, K.R. *User's Manual for Isoplot/Ex Version 3.00, a Geochronological Toolkit for Microsoft Excel*; Berkeley Geochronology Center Special Publications: Berkeley, CA, USA, 2003; Volume 4.
32. Stacey, J.S.; Kramers, J.D. Approximation of Terrestrial Lead Isotope Evolution by a Two-Stage Model. *Earth Planet Sci. Lett.* **1975**, *26*, 207–221. [[CrossRef](#)]
33. Doroshkevich, A.G.; Veksler, I.V.; Klemm, R.; Khromova, E.A.; Izbrodin, I.A. Trace-Element Composition of Minerals and Rocks in the Belaya Zima Carbonatite Complex (Russia): Implications for the Mechanisms of Magma Evolution and Carbonatite Formation. *Lithos* **2017**, *284–285*, 91–108. [[CrossRef](#)]
34. Sun, S.-s.; McDonough, W.F. *Chemical and Isotopic Systematics of Oceanic Basalts: Implications for Mantle Composition and Processes*; Geological Society, London, Special Publications: London, UK, 1989; Volume 42, pp. 313–345. [[CrossRef](#)]
35. Yarmolyuk, V.V.; Kuzmin, M.I.; Ernst, R.E. Intraplate Geodynamics and Magmatism in the Evolution of the Central Asian Orogenic Belt. *J. Asian Earth Sci.* **2014**, *93*, 158–179. [[CrossRef](#)]
36. Prokopyev, I.R.; Doroshkevich, A.G.; Ponomarchuk, A.V.; Kruk, M.N.; Izbrodin, I.A.; Vladykin, N.V. Geochronology of the Alkaline-Ultra-Basic Carbonatite Complex Arbarastakh (Aldan Shlied, Yakutia): New Ar-Ar and U-Pb Data. *Geosfernye Issled.* **2022**, *4*, 48–66. [[CrossRef](#)]
37. Nozhkin, A.D.; Turkina, O.M.; Bayanova, T.B.; Berezhnaya, N.G.; Larionov, A.N.; Postnikov, A.A.; Travin, A.V.; Ernst, R.E. Neoproterozoic Rift and Within-Plate Magmatism in the Yenisei Ridge: Implications for the Breakup of Rodinia. *Russ. Geol. Geophys.* **2008**, *49*, 503–519. [[CrossRef](#)]
38. Vernikovskaya, A.E.; Vernikovskiy, V.A.; Sal'nikova, E.B.; Kotov, A.B.; Kovach, V.P.; Travin, A.V.; Wingate, M.T.D. A -Type Leucogranite Magmatism in the Evolution of Continental Crust on the Western Margin of the Siberian Craton. *Russ. Geol. Geophys.* **2007**, *48*, 3–16. [[CrossRef](#)]
39. Gladkochub, D.P.; Mazukabzov, A.M.; Stanevich, A.M.; Donskaya, T.V.; Motova, Z.L.; Vanin, V.A. Precambrian Sedimentation in the Urik-Iya Graben, Southern Siberian Craton: Main Stages and Tectonic Settings. *Geotectonics* **2014**, *48*, 359–370. [[CrossRef](#)]
40. Ernst, R.E.; Gladkochub, D.P.; Soderlund, U.; Donskaya, T.V.; Pisarevsky, S.A.; Mazukabzov, A.M.; Bilali, H.E. Identification of the ca. 720Ma Irkutsk LIP and its plume centre in southern Siberia: The initiation of Laurentia-Siberia separation. *Precambrian Res.* **2023**, *394*, 107111. [[CrossRef](#)]

**Disclaimer/Publisher's Note:** The statements, opinions and data contained in all publications are solely those of the individual author(s) and contributor(s) and not of MDPI and/or the editor(s). MDPI and/or the editor(s) disclaim responsibility for any injury to people or property resulting from any ideas, methods, instructions or products referred to in the content.